Vascular remodelling in idiopathic pulmonary fibrosis patients and its detrimental effect on lung physiology: potential role of endothelial-to-mesenchymal transition

Archana Vijay Gaikwad[1,2], Wenying Lu[1,2], Surajit Dey[1], Prem Bhattarai[1], Collin Chia[1,3], Josie Larby[1,3], Greg Haug[1,3], Stephen Myers[1], Jade Jaffar[4,5], Glen Westall[4,5], Gurpreet Kaur Singhera[6,7], Tillie-Louise Hackett[6,7], James Markos[1,3], Mathew Suji Eapen[1,2,8] and Sukhwinder Singh Sohal[1,8]

[1]Respiratory Translational Research Group, Dept of Laboratory Medicine, School of Health Sciences, College of Health and Medicine, University of Tasmania, Launceston, TAS, Australia. [2]National Health and Medical Research Council (NHMRC) Centre of Research Excellence (CRE) in Pulmonary Fibrosis, Respiratory Medicine and Sleep Unit, Royal Prince Alfred Hospital, Camperdown, NSW 2050, Australia. [3]Dept of Respiratory Medicine, Launceston General Hospital, Launceston, TAS, Australia. [4]Dept of Allergy, Immunology and Respiratory Medicine, The Alfred Hospital, Melbourne, VIC, Australia. [5]Dept of Immunology and Pathology, Monash University, Melbourne, VIC, Australia. [6]Dept of Anaesthesiology, Pharmacology and Therapeutics, University of British Columbia, Vancouver, BC, Canada. [7]Centre for Heart Lung Innovation, St Paul's Hospital, Vancouver, BC, Canada. [8]Equal contributors.

Corresponding author: Sukhwinder Singh Sohal (sssohal@utas.edu.au)

Shareable abstract (@ERSpublications)
Pulmonary arterial remodelling occurs in IPF patients, affects lung function and may exaggerate pulmonary hypertension. Endothelial-to-mesenchymal transition appears decisive with vascular changes and could be a novel therapeutic target for IPF. https://bit.ly/3GG3qBa

Cite this article as: Gaikwad AV, Lu W, Dey S, *et al*. Vascular remodelling in idiopathic pulmonary fibrosis patients and its detrimental effect on lung physiology: potential role of endothelial-to-mesenchymal transition. *ERJ Open Res* 2022; 8: 00571-2021 [DOI: 10.1183/23120541.00571-2021].

Received: 30 Sept 2021
Accepted: 10 Jan 2022

Abstract

Background Idiopathic pulmonary fibrosis (IPF) is a progressive, irreversible fibrotic interstitial lung disease. We performed size-based quantitation of pulmonary arterial remodelling in IPF and examined the role of endothelial-to-mesenchymal transition (EndMT) and effects on lung physiology.

Methods Resected lung tissues from 11 normal controls (NCs), and 13 IPF patients were differentially stained using the Movat Pentachrome technique. Size-based classification for pulmonary arteries was conducted in NC and IPF tissues. For each pulmonary artery, arterial size, luminal diameter, thickness of the intima, media and adventitia, and elastin deposition were quantified using Image ProPlus7.0 software. In addition, immunohistochemical staining was performed for EndMT markers and collagen.

Results Large and medium-size arterial numbers were significantly reduced in IPF compared to NCs ($p<0.0001$). Intima thickness was highest in the arterial range of 200–399 µm and 600–1000 µm ($p<0.0001$), while medial and adventitial thickness was significant across 200–1000 µm ($p<0.05$) compared to NC. Medial thickness was found to significantly affect the diffusing capacity of the lungs for carbon monoxide (D_{LCO}) ($r=-0.8$, $p=0.01$). Total arterial elastin in IPF was higher across all arterial ranges except 100–199 µm in IPF than in NC, with the greatest differences in 200–399 µm ($p<0.001$) and 600–1000 µm ($p<0.001$). Total elastin also negatively correlated with D_{LCO} ($r'=-0.63$, $p=0.04$) in IPF. An increase in EndMT markers and collagen type I/ IV was observed.

Conclusions This is the first study demonstrating size-based differences in pulmonary arteries in IPF and its detrimental effect on lung physiology. The process of EndMT might be central to these vascular remodelling changes and could be a potential novel therapeutic target.

Introduction

Idiopathic pulmonary fibrosis (IPF) is a progressive chronic interstitial lung disease associated with irreversible lung fibrosis. IPF is a deadly disease, with mortality rates averaging 3.8 years from diagnosis [1, 2]. Currently, IPF affects >3 million people worldwide, which forms a substantial burden on healthcare [3]. Honeycombing and usual interstitial pneumonia (UIP) are some of the common

observations of IPF lung when detected through high-resolution computed tomography [4]. Despite unknown aetiology, environmental, microbial factors and genetic susceptibility are associated with IPF pathogenesis [1, 4]. IPF pathology results from repeated injury to the lung interstitium, causing aberrant repair, leading to intense interstitial fibrosis and restricted gas exchange [5]. Several cells, including alveolar type II pneumocytes, endothelial cells, pericytes, fibrocytes, macrophages and mast cells, are crucial contributors to IPF pathogenesis. These cells promote the accumulation and proliferation of fibroblasts through several as yet undeciphered mechanisms and uneven deposition of extracellular matrix (ECM), culminating in irreversible lung parenchyma scarring and damage [6].

IPF patients are prone to abnormal structural changes in the pulmonary arteries, leading to pulmonary hypertension (PH) [7]. Past findings suggest lower blood vessel formation in fibrotic *versus* non-fibrotic areas, displaying considerable vascular heterogeneity across the IPF lung [8, 9]. Abnormal structural modifications of the vasculature such as complete occlusion or narrowing of the vessels by scarred tissues, plexiform lesions, proliferative intima and thickening of smooth muscle layers are some of the mainstays of IPF pathology [8, 10]. Interestingly, the low diffusing capacity of the lungs for carbon monoxide (D_{LCO}) observed in IPF patients is also linked to PH development, a comorbidity observed in 30–80% of IPF patients [11]. Colombat *et al*. [12] suggested that occlusive venopathy in the non-fibrotic area of IPF lungs caused a reduction in pulmonary capillary blood volume, which was linked to lower D_{LCO} in IPF-PH patients [13]. Furthermore, vascular remodelling was also observed to affect forced vital capacity (FVC) in IPF patients [14], though some studies have reported otherwise [11, 15].

Currently, there is little evidence on systematic morphometric analysis of arterial vascular remodelling in patients with IPF. For example, Parra *et al.* [14] morphometrically evaluated the internal luminal area and the perimeter of medium and large arteries in lung tissue from IPF patients. They suggested significant links between histological UIP patterns and vascular remodelling changes. Decreasing internal luminal area and increasing wall thickness of both medium and large arteries were mainly noted; but the study was semiquantitative [14]. A more recent study by Kinoshita *et al*. [16] used broadly classified arterial ranges to identify increases in individual layer thickness in IPF and idiopathic pleuroparenchymal fibroelastosis patients compared to control lungs tissues. The study, however, lacked association with physiological outcomes.

In the current study, we employed a comprehensive size-based classification approach to study normal and IPF arteries, and we provided data on absolute counts against a cohort of normal healthy controls. In addition, we analysed the thickness of each layer within arteries and have studied their effects on physiological function such as FVC, D_{LCO} and smoking history in IPF patients. Our data indicate that increased deposition of elastin and collagen types I and IV could contribute to the arterial thickness in IPF lung. Finally, we illustrate the possible role of endothelial-to-mesenchymal transition (EndMT) activity in vascular remodelling.

Material and methods

Study population

Explant human lung tissues from 13 patients diagnosed with IPF were obtained during lung transplantation (Alfred Health Biobank Melbourne, ethics ID: 336–13); none were on anti-fibrotic treatment. All patients had pathologist-verified histopathology reports of UIP. In addition, tissues from 11 healthy normal control (NC) subjects consisting of small airways and parenchymal areas were provided by James Hogg Lung Registry, the University of British Columbia (ethics ID: H00-50110). This cohort consisted of patients who had died of causes other than pulmonary diseases. Detailed subject demographic information is provided in table 1. All functional data were collected before the lung transplantation.

Movat's Pentachrome staining

Formalin-fixed, paraffin-embedded 3.5-micron tissue sections were cut. First, dewaxing of the tissue sections was done in xylene twice for 3 min, followed by gradual hydration using 100%, 95%, 70% ethanol, and running tap water. Next, tissue sections were stained using a Movat Pentachrome staining kit (Modified Russell-Movat-ab245884; Abcam, Melbourne, Australia) as per manufacturer instructions. The staining differentiates arterial structural morphology based on colour, such as collagen (yellow to red), elastin (black-blue) and nuclei (blue), muscle (red), mucin (bright blue) and fibrin (bright red) (figures 1 and 2).

Immunohistochemical staining for mesenchymal markers

Lung tissue sections were deparaffinised in xylene and antigen retrieval carried out using target retrieval citrate buffer pH 6.0 (Dako S2369) for 15 min. Tissues were immunostained with polyclonal rabbit anti-human S100A4 (1:1000; Dako A5114), mouse monoclonal VE-cadherin (CD144) (1:150;

TABLE 1 Subject demographics and clinical characteristics

	Normal control	IPF
Total number n	11	13
Age years	41±15.1	64±5.06
Sex (F/M) n	6/5	6/7
Body mass index kg·m^{-2}	NA	26.69±3.03
Smoking status: current/ex-smoker/never-smoker n	Nonsmokers	0/7/6
Smoking pack-years		20.84±23.16
Lung physiology		
FEV_1 L		1.70±0.40
FEV_1 % predicted		60.17±12.22
FVC L		1.97±0.51
FVC % predicted		53.5±12.98
D_{LCO} mL·min^{-1}·mmHg^{-1}		5.91±2.92
D_{LCO} corrected % predicted		25.85±15.30

Values given as mean±SD unless otherwise stated. IPF: idiopathic pulmonary fibrosis; F: female; M: male; NA: not available; FEV_1: forced expiratory volume in 1 s; FVC: forced vital capacity; D_{LCO}: diffusing capacity of the lungs for carbon monoxide.

Thermofisher 14144982), vimentin, monoclonal mouse (1:200; Dako M7020), mouse monoclonal anti-N-cadherin (1:100; Abcam ab98952), monoclonal mouse anti-α-SMA (1:500, M0851, Dako), collagen type I (1:200, Abcam ab34710), rabbit polyclonal and collagen type IV (1:200, Abcam ab6586), rabbit polyclonal for 60 min followed by secondary HRP rabbit/mouse antibodies (Dako K5007) treatment for a further 30 min. The protein markers were visualised as brown after adding DAB substrate and counterstained for the nucleus with haematoxylin.

Pulmonary arterial, classification and counts

All images were captured using a Leica DM 500 microscope and Leica IC50W digital camera. Pulmonary arteries were first distinguished for morphometric analysis based on their rounded structure and thickness, with veins being thinner and elongated (figure 1a). The pulmonary arteries also had at least two defined elastin layers, while veins only had a single layer.

For arterial classification, measurements for at least five arteries of each size were carried out. Each arterial image from NC and IPF tissues was taken with a 4× objective following a vertical uni-direction, avoiding overlap. External length (one end to the other end of adventitia) and luminal length (one end to another end of intima layer margin) were measured (figure 1b) using measurement tools in the image ProPlus 7.0 software. Based on the size measurements, arteries were segregated into six groups, 100–1000 µm, interspaced at 100 µm, and total arterial length to luminal length ratios were calculated to determine the degree of vascular remodelling in IPF (figure 1b). In addition, the arterial numbers per mean per cent of tissue density were counted for all classified arterial sizes in IPF and NC.

Pulmonary total arterial and layer thickness measurement

The length of all three layers of arteries represented the total arterial thickness. To better assess arterial thickness across arterial sizes, separate magnifications were used; for instance, 63× objective for smaller 100–199 µm arteries, 40× for 200–399 µm, 20× for 400–599 µm and 10× for 600–1000 µm respectively. Similar magnifications were used to quantify thickness of individual layers. Subsequently, non-overlapping images were taken for all arterial sizes, and five images per arterial size per subject were randomly selected using an online random number generator. All the analysis was done with an observer (A.V.G.) blinded to subject and diagnosis.

Strategies for arterial thickness measurement were used as previously described [17]. In brief, the area of interest from each layer was manually drawn using imaging software tools. For intima measurements, thickness measurements from the outer luminal to the inner elastin layer were considered. Media layer thickness included the external layer of the inner elastin membrane and internal lining of the external elastin membrane, while areas from the media's external elastin layer to the arteries outermost connective tissue were considered adventitial thickness measurements. Based on arterial orientation, a horizontal,

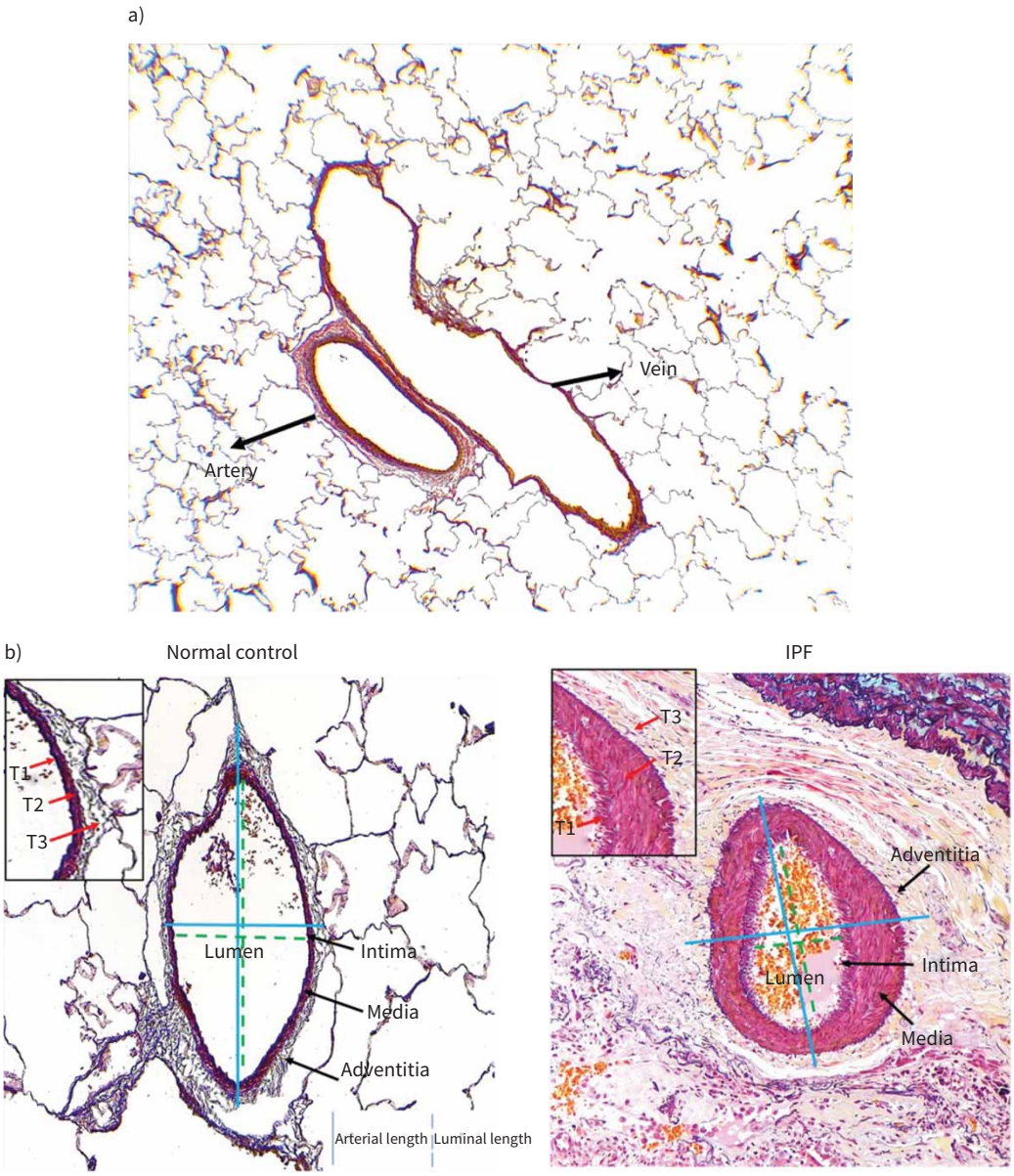

FIGURE 1 a) Illustration of the normal pulmonary artery and vein structure stained with Movat Pentachrome (4× magnification). The pulmonary arteries are well rounded in structure, while veins are elongated and irregular. b) Movat Pentachrome-stained normal control and idiopathic pulmonary fibrosis (IPF) of pulmonary arteries' external and luminal length measurement (20× magnification). External length is measured from one end to the other end of the adventitia layer margin crossing the middle of the lumen, while the luminal length was measured from one end to another end of the intima layer margin. In the inset are layers of various thickness (T1 – intima, T2 – media and T3 – adventitia).

vertical or curved tool was selected using the software measurement tools, and the average distance between the selected layer margins was calculated using an automated distance calculator programme within the image ProPlus 7.0 software.

Pulmonary arterial elastin measurement

Image acquisition and randomisation were carried out similarly to thickness measurements. For total arterial measurements, the start of the outer end of the intima facing the lumen to the outer border of adventitia was manually selected using imaging software. For quantification of elastin, the total dark object was counted from the area of interest, and then elastin colour (black to blue/black) from the area of interest

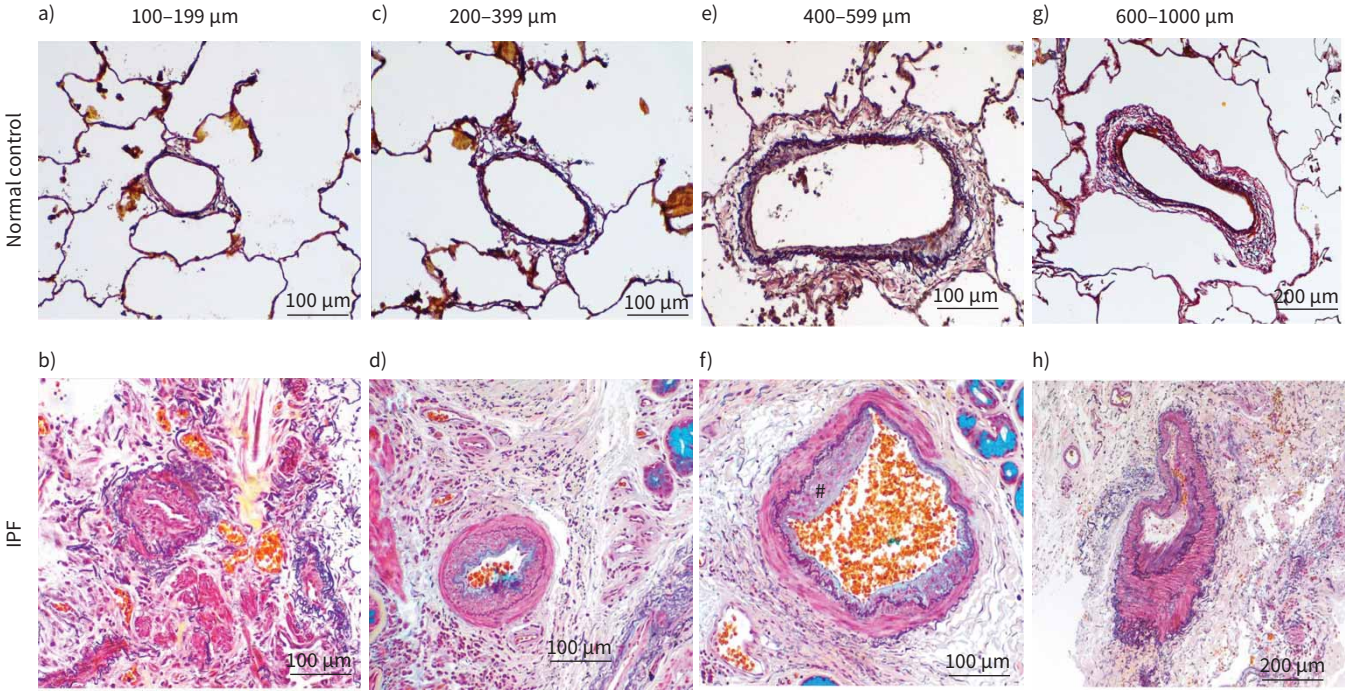

FIGURE 2 Representative images of Movat Pentachrome-stained pulmonary artery sizes for normal control and idiopathic pulmonary fibrosis (IPF): a, b) 100–199 µm, c, d) 200–399 µm, and e, f) 400–599 µm (20× magnification), and g, h) 600–1000 µm (10× magnification). The prominent intimal thickening and luminal narrowing in IPF patients across various sizes are noted. Also noted is the arterial adventitia area merging into the surrounding lung tissues in IPF patients. #: plexiform in part f.

was counted. A similar strategy was used to measure intima, media and adventitia layer elastin. Percentage elastin was calculated using the following formula:

$$\text{Elastin in each arterial layer} = \left(\frac{\text{number of selected colour objects from the area of interest}}{\text{total number of the dark objects from the area of interest}}\right) \times 100$$

Statistical analysis

All cross-sectional data were tested for their normal distributions using the D'Agostino–Pearson omnibus normality test. Analyses of variance were performed using ordinary one-way ANOVA using Bonferroni multiple comparison tests, which compared mean and standard deviation across all the groups of interest; specific group differences with correction for multiple comparisons were assessed using Dunn's test. Finally, for multi-variable correlations, we performed regression analyses using Spearman's rank test. All analysis was done using GraphPad prismV9, with a p-value $\leqslant 0.05$ being considered significant.

Results

Morphological assessment of pulmonary arteries

Large and medium-size arterial numbers were significantly reduced in IPF compared to NC. Compared to arteries in control lungs, patients with IPF showed structural changes such as endothelial proliferation into the lumen, muscular hypertrophy of the intima and medial layer, proliferative intima and plexiform lesions. Also, excessive collagen and elastin deposition at adventitia was observed. Some of the arteries were completely remodelled and indistinguishably merged into surrounding tissues. Our data implicate that increased elastin and collagen deposition could contribute to the arterial thickness in IPF lung (figure 2).

Arterial structural changes and their number

A significant decrease in arterial numbers was observed across medium and larger classified arterial ranges, *i.e.* 200–1000 µm range. Smaller artery numbers also trended lower in IPF but were

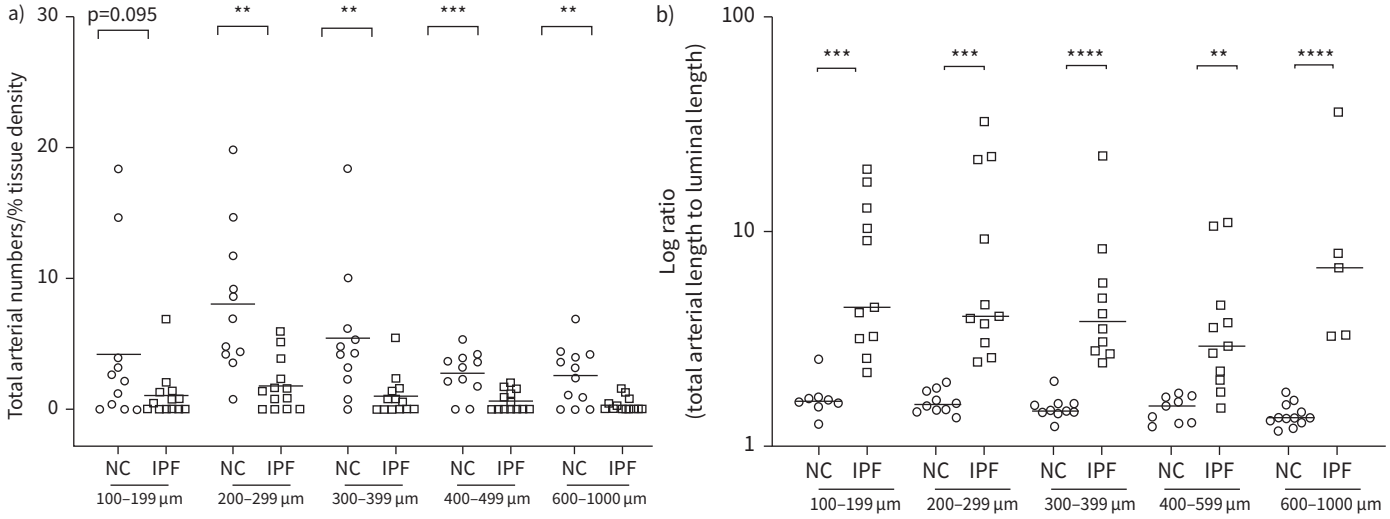

FIGURE 3 a) Quantitative assessment of the total number of arteries in idiopathic pulmonary fibrosis (IPF) and normal control (NC) across classified arterial sizes and b) arterial length to luminal length log ratio of pulmonary arteries across the classified arterial sizes of IPF compared to NC. Data are presented as log ratio with unpaired t-test between each arterial classified size for NC and IPF. **p<0.01, ***p<0.001, ****p<0.0001 was considered significant.

non-significant compared to NC (figure 3a). The differences in total arterial length to lumen ratios in medium to larger 300–399 µm and 600–1000 µm size (p<0.0001) was more significant than 100–199 µm and 200–299 µm (p<0.001) arterial ranges compared to NC (figure 3b).

We analysed relationships between arterial number, total arterial length to lumen ratios and D_{LCO}. We noted that total arterial number positively correlated with D_{LCO} % predicted (r'=0.56, p<0.05) (figure 4a), while the increase in arterial length to luminal ratios negatively correlated with D_{LCO} % predicted (r'=−0.61, p=0.03) (figure 4b). Further, we also observed no significant differences between total arterial length to lumen ratios for arteries from fibrosed and non-fibrosed areas in IPF tissues (figure 4c).

Total arterial and layer thickness in IPF patients

Thickness was measured across all the three arterial zones intima, media and adventitia in NC and IPF (figure 5a, b). Compared to NC, a two-fold increase in total thickness was found across arterial sizes, except the 100–199 µm range, wherein trends were higher, though insignificantly (figure 5c). Among

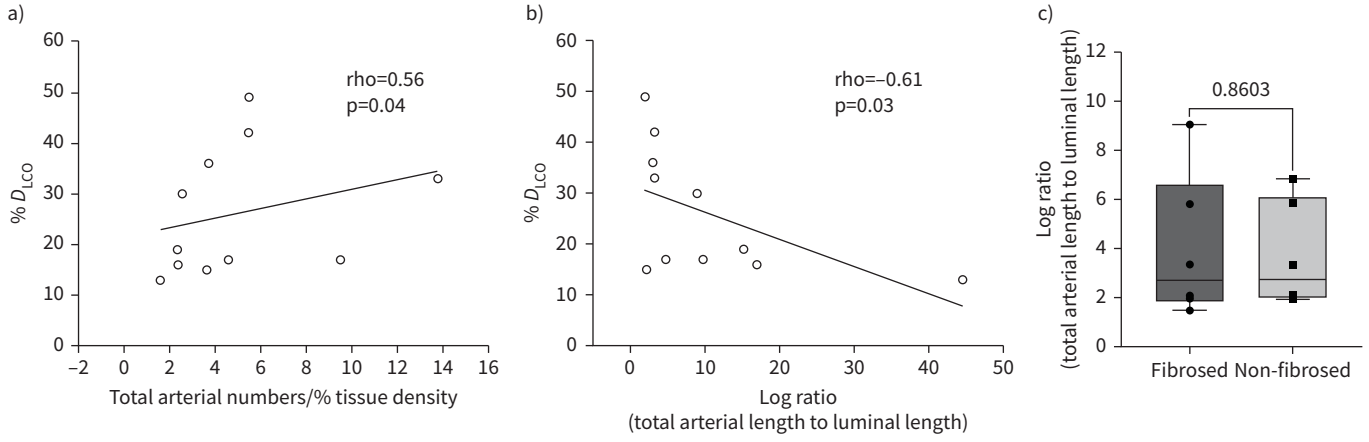

FIGURE 4 Correlations between a) total arterial numbers/mean per cent tissue density and % diffusing capacity of the lungs for carbon monoxide (D_{LCO}); b) total arterial length to luminal length log ratio and % D_{LCO}; and c) total arterial length to luminal length ratio for arteries from fibrosed and non-fibrosed area in idiopathic pulmonary fibrosis.

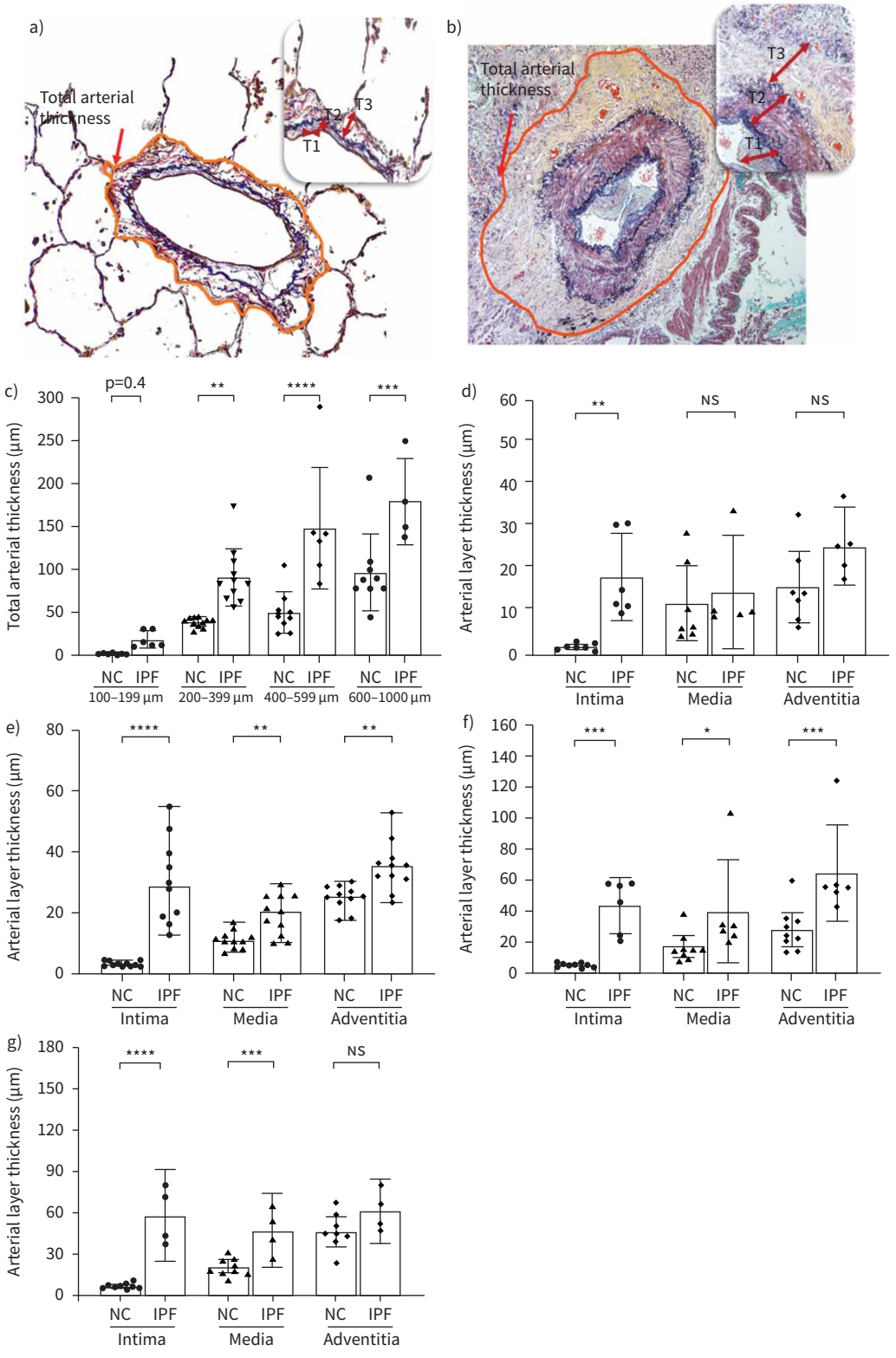

FIGURE 5 a, b) Arterial layer thickness measurement strategy in normal control (NC) and idiopathic pulmonary fibrosis (IPF). Total arterial thickness was measured by selecting total arterial circumference. Insets show layers of various thickness (T1 – intima, T2 – media and T3 – adventitia) thickness. Morphometric changes in arterial layers among c) total arterial thickness across arterial size 100–1000 µm, d) 100–199 µm, e) 200–399 µm, f) 400–599 µm and g) 600–1000 µm. All data are presented as multiple comparisons with ordinary one-way ANOVA. *p<0.05, **p<0.01, ***p<0.001, ****p<0.0001 was considered significant. NS: nonsignificant.

individual arterial layers, intima showed a more significant fold difference in IPF than NC compared to media and adventitia. Intima was thicker across all measured arterial ranges in IPF patients, with greater significance observed in the arterial range of 200–399 µm and 600–1000 µm ($p<0.0001$), respectively, compared to NC (figure 5d–g). Within lower arterial ranges, both medial and adventitial thickness was distinguishably smaller in NC and IPF; however, the larger arterial range had significant increases in media with the greatest difference being in 600–1000 µm ($p<0.001$) and adventitia in 400–599 µm ($p<0.001$) in IPF arteries than NC.

Elastin deposition in arterial layers

The Movat Pentachrome stained elastin dark blue (figure 6a, b). In NC, elastin structures were well defined with inner and outer boundaries surrounding the media smooth muscle layer (figure 6a); however, elastin in IPF was disintegrated and scattered across and within the various layers (figure 6b). Quantitative analysis of the total arterial per cent elastin was significant across arterial ranges in IPF compared to NC except for 100–199 µm. The median value of per cent elastin in IPF subjects was 20% in small and mid-sized arteries, while larger arteries had close to 40% (figure 6c). In comparison, NC had significantly lower total elastin ranging from 5–10% across arterial sizes (figure 6c). Similar trends were observed in individual arterial layer analysis of elastin, with consistent increases seen across mid (200–399 µm ($p<0.001$), 400–599 µm ($p<0.01$)) and larger arteries (600–1000 µm; $p<0.001$); however, smaller arteries showed lower significance, probably due to considerable variability observed in both IPF and NC (figure 6d–g).

Arterial remodelling impact on lung physiology

We analysed relationships between arterial thickness, elastin deposition and lung physiological parameters through a multi-variable correlation matrix. We identified that both total thickness and total per cent elastin showed a significant negative correlation to D_{LCO} % predicted ($r'= -0.75$, $p=0.01$) and ($r'= -0.46$, $p=0.09$), respectively (figure 7a, c). Individual layer thickness negatively correlated with D_{LCO}; intima thickness *versus* D_{LCO} % predicted ($r'= -0.57$, $p=0.05$); media thickness *versus* D_{LCO} % predicted ($r'= -0.84$, $p=<0.001$) and adventitia thickness *versus* D_{LCO} % predicted ($r'= -0.75$, $p\leqslant0.01$). The total and individual layer thickness negatively correlated to FVC (L) insignificantly (figure 7b). Similar to total elastin, individual layers elastin also showed negative correlations D_{LCO} % predicted ($r'= -0.31$, $p=0.17$) for intima, D_{LCO} % predicted ($r'= -0.21$, $p=0.27$) for media and D_{LCO} (%) predicted ($r'= -0.26$, $p=0.22$) for adventitia (figure 7d). Smoking (pack-years) affected both total and individual layer thicknesses and elastin deposition in IPF patients.

The correlation matrix between arterial elastin and thickness showed increased elastin percentage in each arterial layer correlated to their corresponding layer thickness (figure 7e).

Descriptive analysis of IPF arteries showed increase in EndMT marker expression

We observed increased expression of mesenchymal biomarkers N-cadherin, S100A4 and vimentin in the arterial layers (intima, media and adventitia) of IPF patients compared to NC, indicating the possible active transition of resident cells into mesenchymal traits (figure 8c–h). Furthermore, in NC, the endothelial VE-cadherin expression was explicitly observed at cell junctions, while in IPF, they were more cytoplasmic (figure 8a, b). We also observed in the arterial layers of IPF patients an increase in myofibroblast marker α-SMA and ECM proteins collagen type I and IV, especially pronounced in intimal areas compared to NC (figure 8i–n). In addition, the staining intensity of collagen type I was more enhanced and widespread across the tissue than collagen type IV, which was artery specific. Also, unlike IPF, the NC subject's collagen type IV was intact within arterial basement membrane (figure 8m, n).

Discussion

This novel study describes size-based morphological characteristics of the arterial vasculature in IPF, performed through systematic classification, using appropriate quantitative measurement strategies. Noticeably, IPF patients had extensive vascular remodelling changes through increased vascular wall thickening and disruptive ECM deposition. Interestingly, these arterial remodelling changes correlated inversely with lung physiological parameters such as D_{LCO} and FVC, and IPF patients with smoking history had worse outcomes. Further, this study highlights a clear possibility that EndMT could have a critical contribution in driving these irreversible remodelling changes for the first time. Finally, the study highlights the noticeable impact of remodelled vasculature on D_{LCO}, indicating PH complications in IPF patients.

The study noted key histopathological remodelling changes in IPF arteries, including extensive luminal occlusion, intimal proliferation, unevenly dispersed elastin fibres, collagen fragmentation and deposition across arterial layers. In addition, the adventitia was repeatedly found to be merged into surrounding

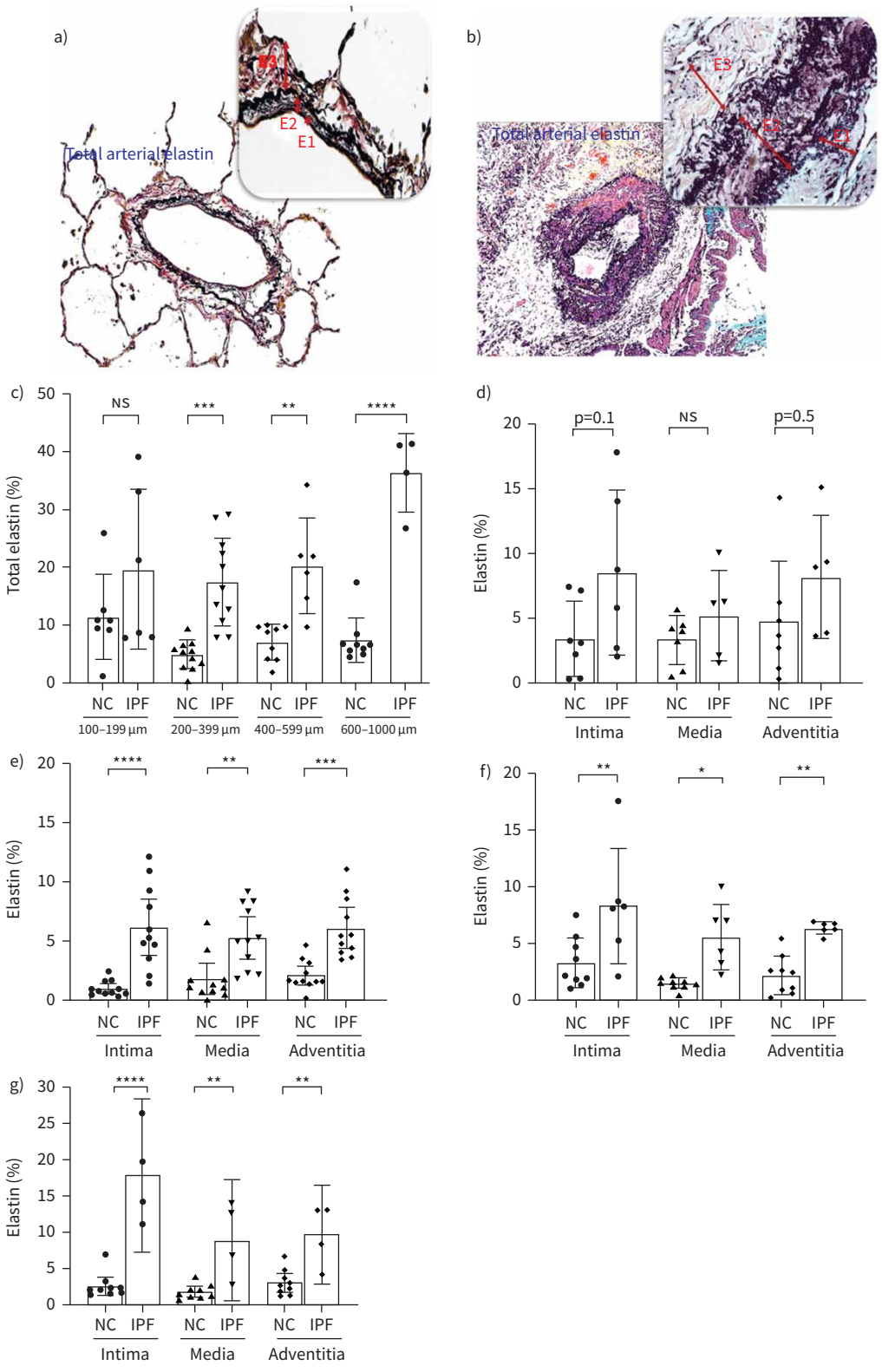

FIGURE 6 a, b) Arterial layer elastin measurement strategy in normal control (NC) and idiopathic pulmonary fibrosis (IPF). The black colour represents the elastin count. Insets show various layers (E1 – intima, E2 – media and E3 – adventitia) of elastin. Morphometric changes in arterial layer elastin among c) total arterial elastin across arterial size 100–1000 µm, d) 100–199 µm, e) 200–399 µm, f) 400–599 µm and g) 600–1000 µm. Arterial elastin is expressed as a percentage. All data are presented as multiple comparisons with ordinary one-way ANOVA. *p<0.05, **p<0.01, ***p<0.001, ****p<0.0001 was considered significant. NS: nonsignificant.

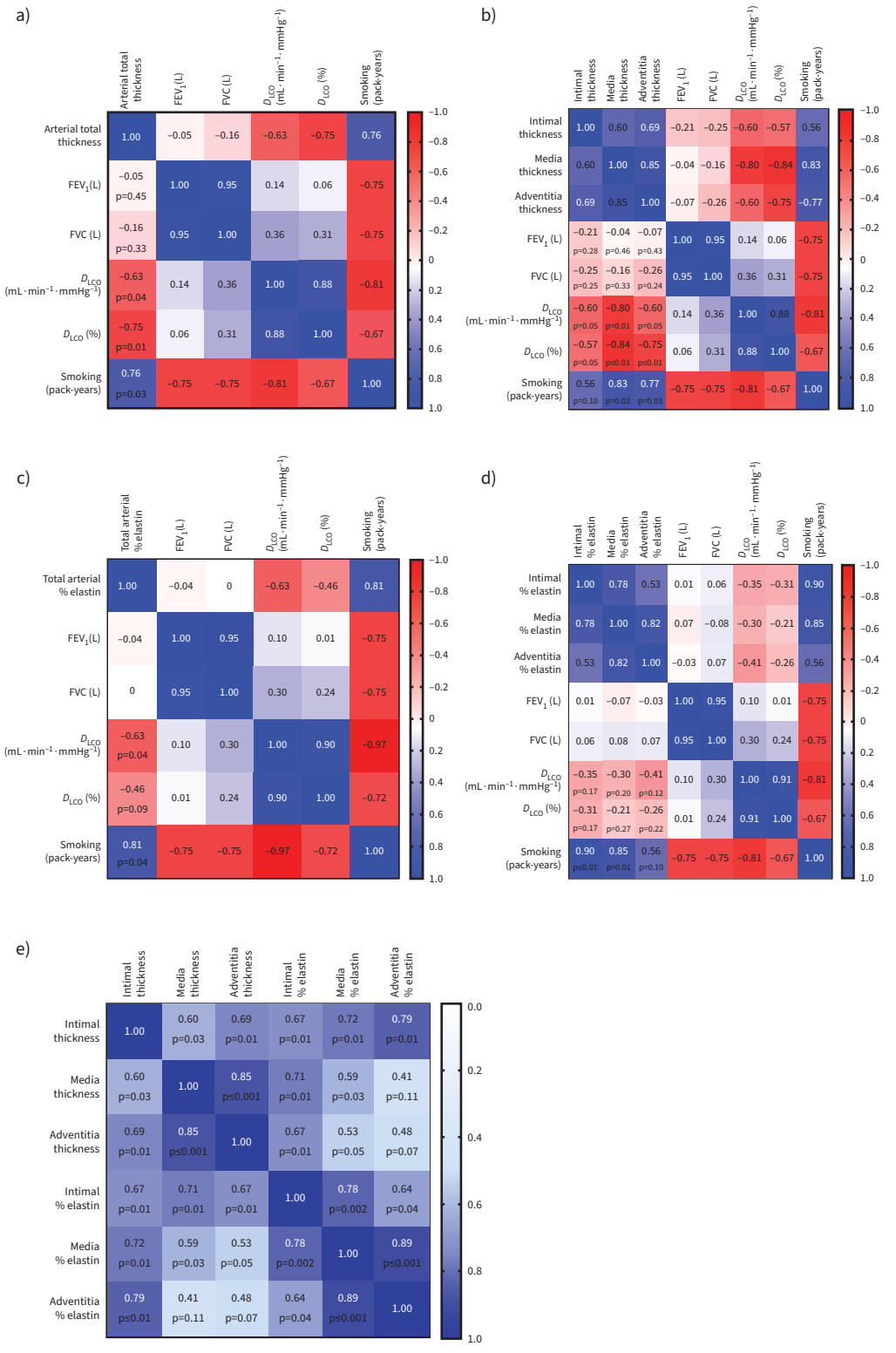

FIGURE 7 Correlations matrix showing the impact on various measured indices on pulmonary function and smoking pack-years: a) pulmonary arterial total thickness, b) arterial individual layer thickness, c) pulmonary arterial total elastin, d) individual arterial layer elastin, and e) correlation between arterial thickness and arterial elastin across each arterial layer. Increased per cent elastin in each layer significantly correlated to their corresponding layer thickness. FEV_1: forced expiratory volume in 1 s; FVC: forced vital capacity; D_{LCO}: diffusing capacity of the lungs for carbon monoxide.

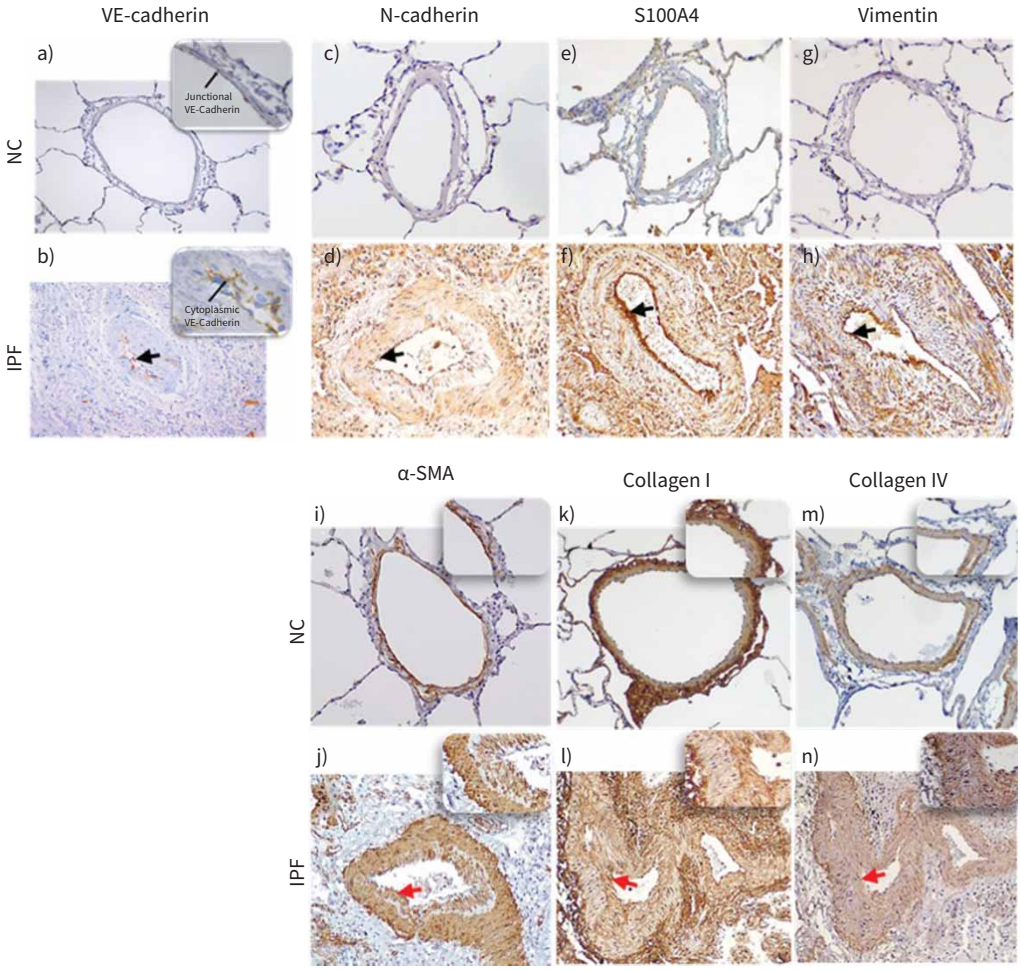

FIGURE 8 Descriptive images of immunohistochemically stained pulmonary arteries for VE-cadherin (magnification 20×): a) normal control (NC), b) idiopathic pulmonary fibrosis (IPF), in insets junctional and cytoplasmic expression of VE-cadherin in NC and IPF, respectively (100×). Staining images for: N-cadherin c) NC and d) IPF (20×); S100A4 e) NC and f) IPF; vimentin g) NC and h) IPF; α-SMA i) NC and j) IPF; collagen-I k) NC and l) IPF; and collagen-IV m) NC and n) IPF (all images taken in 20× magnification for medium-size arteries). The black arrows indicate mesenchymal protein expression in the intima, and the red arrows indicate α-SMA+ myofibroblast (in inset intima) and ECM protein: collagen I and collagen IV deposition (in inset intima).

fibrotic areas. Such features are classically reminiscent of arteries in IPF lungs and very similar as noted in PH-COPD and PH-IPF lung [18] pathology, suggesting a strong relationship between the two pathologies [12, 18]. Furthermore, we identified regression in numbers of medium and large muscular arteries in IPF patients, likely resulting from intense fibrotic remodelling damage or lack of physical space for further arterial expansion. Previous similar findings of such arterial obliteration have been featured in emphysema patients with severe PH [19]. Interestingly, our observation of a much lower decline in smaller arteries illustrates heterogeneity in arterial formation. Earlier findings on vascular formation in IPF are contradictory, with Keane *et al*. [20] demonstrating augmented angiogenic activity. In contrast, others have documented a decline in vessel formation, identified primarily through lower vascular endothelial growth factor levels in bronchoalveolar lavage of IPF patients [21, 22]. Also, our study found no apparent differences between total arterial thickness across the sizes in fibrotic areas and the more normal non-fibrotic areas. Although only a few areas with corresponding arterial sizes were available, our analysis suggests that such remodelling change, at least in the late stage of IPF, does not differ based on the fibrotic status and would represent the pathological changes in their entirety. Future studies with tissues from comparing early and late-stage fibrotic *versus* non-fibrotic areas could better predict pathological arterial remodelling.

The arterial architecture comprises three layers, the inner intima constituting endothelial cells, the medial smooth muscle layer bounded by elastin laminas and the outer adventitial, mainly connective tissues [23]. Any configurational change to these layers affects the overall oxygenation, leading to severe hypoxic conditions. Our assessment of the arteries revealed thickening of the layer across arterial sizes in IPF lungs compared to healthy controls. Specifically, our data suggest a more considerable intimal thickening than the media and adventitia layer across the arterial sizes than seen in healthy subjects. Few previous studies have made such extensive and critical analyses of IPF arteries. Our findings are in contrast to a previous study by Kinoshita *et al*. [16], who identified significantly more thickening in adventitia than in intima and media in their patient cohort, and, to an extent, are in concurrence with findings by Hoffman *et al*. [24] who identified an increase in intima and media but not in adventitia in the IPF-PF cohort of patients. However, both studies lacked essential correlation to human lung physiological parameters, which is critical in the clinical understanding of disease progression and has been addressed in the current study.

The heightened activity of the endothelium in the intima and their aggressive encroachment into luminal space can be attributed to their transformative ability into a more proliferative phenotype; however, molecular exploration into such endothelial cell changes in IPF is still warranted [24]. Several growth factors and signalling mechanisms, including transforming growth factor-β, hedgehog (SHH) and notch, are highly active in IPF tissues and are crucial to EndMT and proliferation [25, 26]. Similar factors could be contributing to medial and adventitial thickening, for which smooth muscle hypertrophy and fibroblast hyperplasia were exhibited in our study of IPF arteries [23, 27]. An interesting study by Arribas *et al*. [28] in a rat hypertension model showed that the adventitial thickening occurred well before changes in intima or media occurred, actively causing arterial remodelling and PH. The inter-dynamics of arterial layers and their cause-and-effect relationship with overall vascular thickening remain underexplored and require further understanding in IPF.

Elastin fibres maintain the structural integrity of the vasculature. In normal arteries, the internal and external elastin laminas consist of mature elastic fibres that offer elasticity to the vascular tissue. Their fragmentation or aberrant deposition can adversely affect elastic recoil and other vascular mechanical properties [29, 30]. Our study identified increased accumulation and elastin breakdown across different arterial layers and sizes in IPF patients. Our data support the observation of Kinoshita *et al*. [16] of medial elastosis in IPF patients; however, unlike their findings, our study showed more significant elastin deposition in the intimal layer than in media and adventitia, especially in medium and large arteries. The increased presence of elastin, either as fragments or elastic laminal thickening, can aid endothelial migration and enhance metalloprotease activities [31, 32]. Minkin *et al*. [33] demonstrated the elastin degradation products such as desmosine and isodesmosine in urine and blood samples from patients diagnosed with pulmonary arterial hypertension (PAH). The presence of elastin fragments in the circulation activates cytokines and associated signalling pathways that can further degrade elastic fibres [31]. Both elastin and collagen contribute to the arterial thickening and PAH development in humans [34]. Poiani *et al*. [35] in hypoxia-induced PH rat models showed increased accumulation of elastin and collagen in pulmonary arteries. Several *in vitro* studies have previously demonstrated that a poor oxygen environment is conducive to fibroblast proliferation and ECM accumulation [36, 37]

Lung physiological tests such as FVC and D_{LCO} are used to assess IPF patient's lung function. In IPF patients, these lung function parameters are adversely affected. Reduced D_{LCO} out of proportion to the underlying pulmonary fibrosis is a sign of concomitant PH [27]. Nadrous *et al*. [38] also observed frequent PH in advanced IPF correlated with low D_{LCO} and low resting and arterial oxygen tension. Our study data confirm significant vascular remodelling changes such as increased arterial thickness, and elastin negatively influenced D_{LCO} and FVC in IPF patients. Reduction in arterial numbers and luminal size was also observed to impact D_{LCO} adversely. Occlusive venopathy has also been observed in non-fibrotic lung areas of IPF patients, suggesting that the reduction in pulmonary capillary blood volume is due to occlusive venopathy and related to low D_{LCO} values in the IPF-PH patients [12]. We also identified that smoking impacted arterial thickness and elastin deposition similar to that reported in COPD patients associated with PH comorbidities [39].

Our descriptive observations indicate the increased presence of mesenchymal cells in the intima, media and adventitia layers, implying mesenchymal transformation in vascular cells [7]. The intimal mesenchymal marker expression was the highest among the three layers, indicating possible endothelial cell transition through the EndMT process [40–43]. In media and adventitia, the presence of mesenchymal cells markers such as N-cadherin, Vimentin and S100A4 was intriguing and pointed towards either resident cell transformation to mesenchymal cells or active inward migration of transitioning endothelial cells; however, these observations need further in-depth verification. Interestingly, we also observed

increased cytoplasmic expression rather than junctional of VE-cadherin in IPF endothelial cells, indicating possible active cellular uptake of this protein. Furthermore, we demonstrate an increase in α-SMA+ expression prominently in the intimal layer of IPF arteries, suggesting inadvertent myofibroblast proliferation. The myofibroblasts are a highly active form of fibroblast known to aberrantly secrete ECM protein, causing thickening and stiffening of tissues [17]. The increase in collagen type I and IV's aberrant and disruptive deposition is possibly linked to αSMA+ myofibroblasts; however, the source of these cells requires further investigation. Together with other cell types, transitioning endothelial cells could majorly contribute to the arterial remodelling and fibrotic pathology observed in IPF. Thus, we postulate the substantial involvement of EndMT in arterial remodelling and its possible role in PH and other lung complications.

A limitation of this study is that the number of IPF and NC samples varied for size-based comparison, as some arterial sizes were not found in IPF and NC tissues. Another limitation is the non-availability of cardiac function data or a clinical diagnosis of PH for the IPF patients studied, and as such, these associations could not be established in this study. However, the negative correlation of vascular remodelling with D_{LCO} indicates possible PH in IPF patients.

In summary, this study provides important morphometric data on the remodelling of muscular arteries in the IPF lung. More importantly, we have identified that such change directly resulted in physiological change, deficient oxygen absorption and reduced lung capacity. EndMT seems central to IPF pathology and could be a novel therapeutic target. Thus, our data would support the need for diagnosis and therapeutic options for vascular remodelling, which might occur with IPF prognosis and future complications.

Provenance: Submitted article, peer reviewed.

Acknowledgements: Archana Vijay Gaikwad, Wenying Lu and Mathew Suji Eapen are thankful to the National Health and Medical Research Council Centre of Research Excellence in Pulmonary Fibrosis (Australia) for the CREATE Fellowship.

Conflict of interest: S.S. Sohal reports personal fees for lectures from Chiesi outside the submitted work. All the other authors do not have any conflict of interest to declare.

Support statement: This work was supported by research grants from Clifford Craig Foundation, Launceston General Hospital and Lung Foundation Australia. Funding information for this article has been deposited with the Crossref Funder Registry.

References

1 Lederer DJ, Martinez FJ. Idiopathic pulmonary fibrosis. *N Engl J Med* 2018; 378: 1811–1823.
2 Eapen MS, Gaikwad AV, Thompson IE, *et al.* The effectiveness of immunosuppressive cyclosporin in attenuating the progression of interstitial lung diseases. *J Thorac Dis* 2019; 11: S1139–S1142.
3 Glassberg MK. Overview of idiopathic pulmonary fibrosis, evidence-based guidelines, and recent developments in the treatment landscape. *Am J Manag Care* 2019; 25: Suppl. 11, S195–S203.
4 Raghu G, Remy-Jardin M, Myers JL, *et al.* Diagnosis of idiopathic pulmonary fibrosis. An official ATS/ERS/JRS/ALAT clinical practice guideline. *Am J Respir Crit Care Med* 2018; 198: e44–e68.
5 Richeldi L, Collard HR, Jones MG. Idiopathic pulmonary fibrosis. *Lancet* 2017; 389: 1941–1952.
6 Bagnato G, Harari S. Cellular interactions in the pathogenesis of interstitial lung diseases. *Eur Respir Rev* 2015; 24: 102–114.
7 Ghigna M-R, Dorfmüller P. Pulmonary vascular disease and pulmonary hypertension. *Diagn Histopathol* 2019; 25: 304–312.
8 Farkas L, Gauldie J, Voelkel NF, *et al.* Pulmonary hypertension and idiopathic pulmonary fibrosis: a tale of angiogenesis, apoptosis, and growth factors. *Am J Respir Cell Mol Biol* 2011; 45: 1–15.
9 Barratt S, Millar A. Vascular remodelling in the pathogenesis of idiopathic pulmonary fibrosis. *QJM* 2014; 107: 515–519.
10 Nathan SD, Shlobin OA, Ahmad S, *et al.* Serial development of pulmonary hypertension in patients with idiopathic pulmonary fibrosis. *Respiration* 2008; 76: 288–294.
11 Lettieri CJ, Nathan SD, Barnett SD, *et al.* Prevalence and outcomes of pulmonary arterial hypertension in advanced idiopathic pulmonary fibrosis. *Chest* 2006; 129: 746–752.
12 Colombat M, Mal H, Groussard O, *et al.* Pulmonary vascular lesions in end-stage idiopathic pulmonary fibrosis: histopathologic study on lung explant specimens and correlations with pulmonary hemodynamics. *Hum Pathol* 2007; 38: 60–65.

13 Sakao S, Tanabe N, Tatsumi K. Hypoxic pulmonary vasoconstriction and the diffusing capacity in pulmonary hypertension secondary to idiopathic pulmonary fibrosis. *J Am Heart Assoc* 2019; 8: e013310.
14 Parra ER, David YR, Costa L, *et al.* Heterogeneous remodeling of lung vessels in idiopathic pulmonary fibrosis. *Lung* 2005; 183: 291–300.
15 Nathan SD, Noble PW, Tuder RM. Idiopathic pulmonary fibrosis and pulmonary hypertension: connecting the dots. *Am J Respir Crit Care Med* 2007; 175: 875–880.
16 Kinoshita Y, Ishii H, Kushima H, *et al.* Remodeling of the pulmonary artery in idiopathic pleuroparenchymal fibroelastosis. *Sci Rep* 2020; 10: 306.
17 Eapen MS, Lu W, Hackett TL, *et al.* Increased myofibroblasts in the small airways, and relationship to remodelling and functional changes in smokers and COPD patients: potential role of epithelial–mesenchymal transition. *ERJ Open Res* 2021; 7: 00876-2020.
18 Heath D, Edwards JE. The pathology of hypertensive pulmonary vascular disease; a description of six grades of structural changes in the pulmonary arteries with special reference to congenital cardiac septal defects. *Circulation* 1958; 18: 533–547.
19 Adir Y, Shachner R, Amir O, *et al.* Severe pulmonary hypertension associated with emphysema: a new phenotype? *Chest* 2012; 142: 1654–1658.
20 Keane MP, Belperio JA, Burdick MD, *et al.* ENA-78 is an important angiogenic factor in idiopathic pulmonary fibrosis. *Am J Respir Crit Care Med* 2001; 164: 2239–2242.
21 Meyer KC, Cardoni A, Xiang Z-Z. Vascular endothelial growth factor in bronchoalveolar lavage from normal subjects and patients with diffuse parenchymal lung disease. *J Lab Clin Med* 2000; 135: 332–338.
22 Tzouvelekis A, Anevlavis S, Bouros D. Angiogenesis in interstitial lung diseases: a pathogenetic hallmark or a bystander? *Respir Res* 2006; 7: 82.
23 Tomashefski JF, Dail DH. Dail and Hammar's Pulmonary Pathology, Vol. 1. New York, Springer, 2008.
24 Hoffmann J, Wilhelm J, Marsh LM, *et al.* Distinct differences in gene expression patterns in pulmonary arteries of patients with chronic obstructive pulmonary disease and idiopathic pulmonary fibrosis with pulmonary hypertension. *Am J Respir Crit Care Med* 2014; 190: 98–111.
25 Gaikwad AV, Eapen MS, McAlinden KD, *et al.* Endothelial to mesenchymal transition (EndMT) and vascular remodeling in pulmonary hypertension and idiopathic pulmonary fibrosis. *Expert Rev Respir Med* 2020; 14: 1027–1043.
26 Liu G, Philp AM, Corte T, *et al.* Therapeutic targets in lung tissue remodelling and fibrosis. *Pharmacol Ther* 2021; 225: 107839.
27 Ruffenach G, Hong J, Vaillancourt M, *et al.* Pulmonary hypertension secondary to pulmonary fibrosis: clinical data, histopathology and molecular insights. *Respir Res* 2020; 21: 303.
28 Arribas SM, Hillier C, González C, *et al.* Cellular aspects of vascular remodeling in hypertension revealed by confocal microscopy. *Hypertension* 1997; 30: 1455–1464.
29 Karnik SK, Brooke BS, Bayes-Genis A, *et al.* A critical role for elastin signaling in vascular morphogenesis and disease. *Development* 2003; 130: 411–423.
30 Roger Parra E, Adib Kairalla R, de Carvalho CRR, *et al.* Abnormal deposition of collagen/elastic vascular fibres and prognostic significance in idiopathic interstitial pneumonias. *Thorax* 2007: 62: 428–437.
31 Cocciolone AJ, Hawes JZ, Staiculescu MC, *et al.* Elastin, arterial mechanics, and cardiovascular disease. *Am J Physiol Heart Circ Physiol* 2018; 315: H189–H205.
32 Skeie JM, Mullins RF. Elastin-mediated choroidal endothelial cell migration: possible role in age-related macular degeneration. *Invest Ophthalmol Vis Sci* 2008; 49: 5574–5580.
33 Minkin R, Grosu H, Tartell L, *et al.* Detection of elastin degradation products in the blood and urine of patients with pulmonary arterial hypertension. *Chest* 2010; 138: Suppl. 4, 891A.
34 Rabinovitch M. Pathobiology of pulmonary hypertension. Extracellular matrix. *Clin Chest Med* 2001; 22: 433–449.
35 Poiani GJ, Tozzi CA, Yohn SE, *et al.* Collagen and elastin metabolism in hypertensive pulmonary arteries of rats. *Circ Res* 1990; 66: 968–978.
36 Das M, Dempsey EC, Bouchey D, *et al.* Chronic hypoxia induces exaggerated growth responses in pulmonary artery adventitial fibroblasts: potential contribution of specific protein kinase c isozymes. *Am J Respir Cell Mol Biol* 2000; 22: 15–25.
37 Falanga V, Kirsner RS. Low oxygen stimulates proliferation of fibroblasts seeded as single cells. *J Cell Physiol* 1993; 154: 506–510.
38 Nadrous HF, Pellikka PA, Krowka MJ, *et al.* The impact of pulmonary hypertension on survival in patients with idiopathic pulmonary fibrosis. *Chest* 2005; 128: Suppl. 6, 616s–617s.
39 Peinado VI, Pizarro S, Barberà JA. Pulmonary vascular involvement in COPD. *Chest* 2008; 134: 808–814.
40 Sohal SS. Endothelial to mesenchymal transition (EndMT): an active process in chronic obstructive pulmonary disease (COPD)? *Respir Res* 2016; 17: 20.
41 Sohal SS. Epithelial and endothelial cell plasticity in chronic obstructive pulmonary disease (COPD). *Respir Investig* 2017; 55: 104–113.

42 Eapen MS, Myers S, Lu W, *et al.* sE-cadherin and sVE-cadherin indicate active epithelial/endothelial to mesenchymal transition (EMT and EndoMT) in smokers and COPD: implications for new biomarkers and therapeutics. *Biomarkers* 2018; 23: 709–711.
43 Eapen MS, Lu W, Gaikwad AV, *et al.* Endothelial to mesenchymal transition: a precursor to post-COVID-19 interstitial pulmonary fibrosis and vascular obliteration? *Eur Respir J* 2020; 56: 2003167.